Yohei Mukai, Takayuki Okamoto, Madoka Taniai, Maki Kawamura, Yasuhiro Abe, Shinsaku Nakagawa, Takao Hayakawa, Satoshi Nagata, Yuriko Yamagata, Tadanori Mayumi, Haruhiko Kamada, Yasuo Tsutsumi					
Takuo Suzuki, Tomoko Mogami, Hiroshi Kawai, Tetsu Kobayashi, Youichi Shinozaki, Yoji Sato, Toshihiro Hashimoto, Yoshinori Asakawa, Kazuhide Inoue, Yasuo Ohno, Takao Hayakawa and Toru Kawanishi	Screening of novel nuclear receptor agonists by a convenient reporter gene assay system using green fluorescent protein derivatives	Phytomedicine		in press	
Tetsuji Hosono, Hiroyuki Mizuguchi, Kazufumi Katayama, Naoya Koizumi, Kenji Kawabata, Teruhide Yamaguchi, Shinsaku Nakagawa, Yoshiteru Watanabe, Tadanori Mayumi, Takao Hayakawa	RNA interference of PPARg using fiber-modified adenovirus vector efficiently suppresses preadipocyte-to-adipocyte differentiation in 3T3-L1 cells	Gene		in press	

Akira HARAZONO, Nana KAWASAKI, Toru KAWANISHI, and Takao HAYAKAWA	Site-specific glycosylation analysis of human apolipoprotein B100 using high-perormance liquid chromatography/electrospray ionization tandem mass spectrometry.	Glycobiology		in press	
Jin YUAN, Noritaka HASHII, Nana KAWASAKI, Satsuki ITOH, Toru KAWANISHI, and Takao HAYAKAWA	Isotope tag method for quantitative analysis of carbohydrates by liquid chromatography/mass spectrometry.	J. Chromatogr. A		in press	
Niimi, S., Harashima, M., Takayama, K., Hara, M., Hyuga, M., Seki, T., Ariga, T., Kawanishi, T., Hayakawa, T.	Thrombomodulin enhances the invasive activity of mouse mammary tumor cells.	J. Biochem		in press	
Niimi, S., Harashima, M., Gamou, M., Hyuga, M., Seki, T., Ariga, T., Kawanishi, T., Hayakawa, T.	Expression of annexin A3 in primary cultured parenchymal rat hepatocytes and inhibition of DNA synthesis by suppression of annexin A3 using RNA interference.	Biol. Pharm. Bull.		in press	
Nasimuzzaman, M., Kuroda, M., Dohno, S., Yamamoto, T., Iwatsuki, K., Matsuzaki, S., Rashel, M., Kumita, W., Mizuguchi, H., Hayakawa, T., Nakamura, H., Taguchi, T., Wakiguchi, H., Imai, S.	Eradication of Epstein-Barr virus episome and associated inhibition of infected tumor cell growth by adenovirus vector-mediated transduction of dominant-negative EBNA1.	Mol. Ther.		in press	

Kawai H., Suzuki T., Kobayashi T., Sakurai H., Ohata H., Honda K., Momose K., Namekata I., Tanaka H., Shigenobu K., Hayakawa T., Kawanishi T.	Simultaneous real-time detection of initiator- and effector-caspase activation by double FRET analysis.	J. Pharmacol. Sci.		in press	
Kanayasu-Toyoda T, Fujino T, Oshizawa,T., Suzuki,T., Nishimaki-Mogami,T., Sato.Y., Sawada,J., Inoue,K., Shudo,K., Ohno,Y., Yamaguchi T	HX531, RXR antagonist, inhibited the 9-cis retinoic acid-induced binding with steroid receptor coactivator-1 using surface plasmon resonance	J. Steroid Biochem Mol		in press	
水口裕之・早川堯夫	ウイルスベクター	Drug Delivery System		印刷中	
水口裕之・川端健二・櫻井文教・早川堯夫	改良型アデノウイルスベクターを用いた造血幹細胞、間葉系幹細胞、ES細胞への高効率遺伝子導入	炎症・再生		印刷中	
Toshie Tsuchiya	A useful marker for evaluating the safety and efficacy of tissue engineered products.	ASTM	STP 1452	254-261	2004
Misao Nagahata, Toshie Tsuchiya et. al	A novel function of N-cadherin and Connexin43 :Marked enhancement of alkaline phosphatase activity in rat calvarial osteoblast exposed with sulfated hyaluronan	Biochem. Biophys. Res. Commun	315(3)	603-611	2004
Haishima Y, Matsuda R, Hayashi Y, Hasegawa C, Yagami T, Tsuchiya T	Risk assessment of di(2-ethylhexyl)phthalate released from PVC blood circuits during hemodialysis and pump-oxygenation therapy.	International Journal of Pharmaceutics	274	119-129	2004
Saifuddin Ahmed, Toshie Tsuchiya	Novel mechanism of tumorigenesis: Increased transforming growth factor-beta 1 suppresses the expression of connexin 43 in BALB/cJ mice after implantation of	J Biomed Mater Res	70	335-340	2004

	poly-L-lactic acid.				
Takeshi Yagami, Yuji Haishima, Toshie Tsuchiya, Akiko Tomitaka-Yagami, Hisao Kano, Kayoko Matsunaga	Proteomic Analysis of Putative Latex Allergens.	Allergy and Immunology	135	3-11	2004
Eiji Okada, Yuka Komazawa, Masaki Kirihara, Hideshi Inoue, Naoki Miyato, haruhiro Okuda, Toshie Tsuchiya, Yoko Ymamakoshi	Synthesis of C60 derivatives for photoaffinity labering	Tetrahedron Letters	45	527-529	2004
Tsuchiya T, Sakai M, Ikeda H, Mashino T, Banu Y	Biocompatible biomaterials for the human chondrocyte differentiation estimated by RT-PCR method	Animal cell technology	13	475-479	2004
Saifuddin Ahmed and Toshie Tsuchiya	Different expression on Gap junctional protein connexin43 in two strains of mice after one-month Implantation of Poly-L-Lactic acid	Animal cell technology	13	481-485	2004
Rahman MS, Banu Y, Matsuoka A, Ichikawa A, Sakai M, Ikeda H, Tsuchiya T	Evaluation of the immuno-protective effects of the new-type of bags using ELISA- and FACS-analysis	Animal cell technology	13	277-280	2004
Atsuko Matsuoka, Toshie Tsuchiya	Gene expression changes in Balb/3T3 transformants induced by poy(L-lactic acid) or polyurethane film	J. Biomed. Mater. Res	68A	376-382	2004
土屋利江	細胞組織医療機器等の製品化のためのガイドライン・環境整備について	高分子	53(3)	144-146	2004
土屋利江	細胞組織医療機器等の品質・安全性確保について	再生医療	3(2)	107-110	2004
土屋利江	バイオマテリアルの安全性について組織工学用材料を中心として	日本再生歯科医学会誌	2	1-8	2004
土屋利江	ティッシュエンジニアリング用マテリアルの製品化条件と国際標準化	再生医療	3(5)	71-75	2004

土屋利江	バイオマテリアルの許認可と留意点	バイオマテリアル-生体材料	22(4)	258-264	2004
Nagahata M, Nakaoka R, Teramoto A, Abe K, Tsuchiya T	he response of normal human osteoblasts to anionic polysaccharide polyelectrolyte complexes.	Biomaterials		in press	
Nakaoka R, Ahmed S, Tsuchiya T	Hydroxy apatite microspheres enhance gap junctional intercellular communication of human osteoblasts composed of connexin 43 and 45.	J. Biomed. Mater. Res. A		in press	
Saifuddin Ahmed, Toshie Tsuchiya and Yutaka Kariya	Studies on the efficacy, safety and quality of the tissue engineered productis: Enhancement of proliferation of Human mesenchymal stem cells by the new polysaccharides.	Animal Cell Technology		in press	
Rumi Sawada, Tomomi Ito, Yoshie Matsuda, and Toshie Tsuchiya	Safety evaluation of tissue engineered medical devices using normal human mesenchymal stem cells.	Animal Cell Technology		in press	
Nasreen Banu, Toshie Tsuchiya, Saifuddin Ahmed, and Rumi Sawada	Studies on the efficacy, safety and quality of the tissue engineered products: Effects of a catalyst used in the synthesis of biodegradable polymer on the chondogenesis of human articular cartilage.	Animal Cell Technology		in press	
Yuping Li, Tsutomu Nagira and Toshie Tsuchiya	Increase of the insulin secretion in hit-t15 cells: Gap Junctional Intercellular communications Enhanced by Hyaluronic Acid.	Animal Cell Technology		in press	
長幡　操、寺本　彰、阿部康次、中岡竜介、土屋利江	ラット頭蓋冠由来骨芽細胞のALPase活性を促進する硫酸化ヒアルロン酸の効果	繊維学会誌		印刷中	

Available online at www.sciencedirect.com
SCIENCE DIRECT®
Biologicals 32 (2004) 139–146
BIOLOGICALS
www.elsevier.com/locate/biologicals

An improved method for detection of replication-competent retrovirus in retrovirus vector products

Eriko Uchida[a,*], Koei Sato[b], Akiko Iwata[b], Akiko Ishii-Watabe[a], Hiroyuki Mizuguchi[a], Mikio Hikata[c], Mitsuhiro Murata[c], Teruhide Yamaguchi[a], Takao Hayakawa[a]

[a]*National Institute of Health Sciences, 1-18-1 Kamiyoga, Setagaya-ku, Tokyo 158-8501, Japan*
[b]*Institute of Saitama Red Cross Center, 398-1 O-aza-narashinden, Kumagaya, Saitama 368-0806, Japan*
[c]*JSR Corporation, Tsukuba Research Laboratories, Miyukigaoka 25, Tsukuba, Ibaraki 305-0841, Japan*

Received 20 February 2004; accepted 19 August 2004

Abstract

Contamination by replication-competent retrovirus (RCR) is one of the most important safety issues of retrovirus vector products for gene therapy clinical research. To improve the sensitivity of RCR detection and to shorten the assay period, we have developed a novel RCR detection method (infectivity RT-PCR method) based on real-time quantitative reverse transcription-polymerase chain reaction (RT-PCR) in combination with virus infection and a novel virus concentration method using polyethyleneimine (PEI)-conjugated magnetic beads. In this method, permissive cells were infected with RCR samples, and amplified RCR in the culture supernatants was adsorbed by PEI-beads. Then RCR RNA extracted from PEI-beads was quantified by real-time RT-PCR. We demonstrated that 1 infectious unit (iu) of RCR spiked in 10^6 cfu/ml of vector products could be detected within 3 days, and the sensitivity for viral detection was increased 3- to 10-fold compared with the direct S + L− assay. By this method, the presence of retroviral vector interfered with RCR detection only slightly. In conclusion, infectivity RT-PCR conducted in conjunction with virus concentration using PEI-beads can detect RCR more sensitively and rapidly than the conventional infectivity assay.

1. Introduction

Retrovirus vectors are widely used in human gene therapy to treat genetic diseases, cancer, and other conditions. The retroviral vector products currently used in gene therapy clinical researches are replication-defective retroviruses, and the primary safety concern associated with the use of retroviral vector products is contamination by replication-competent retrovirus (RCR). RCR is the major risk factor for insertional mutagenesis, and exposure to retrovirus vector contaminated with a high titer of RCR has been shown to lead to lymphoma in rhesus monkeys [1].

The most likely source of RCR is the vector-packaging sequence. Since RCR can arise by homologous recombination during the production of retroviral vector supernatants, sensitive assays for the screening of RCR in vector products are required. The U.S. Food and Drug Administration (FDA) has developed guidelines for testing of RCR in clinical grade vectors and transduced cells, as well as for monitoring patients

Abbreviations: RCR, replication-competent retrovirus; RT-PCR, reverse transcription-polymerase chain reaction; PEI, polyethyleneimine; iu, infectious units; cfu, colony forming units; MLV, murine leukemia virus; AMLV, amphotropic MLV.

* Corresponding author. Tel./fax: +81 3 3700 9217.
E-mail address: uchida@nihs.go.jp (E. Uchida).

1045-1056/04/$30.00 © 2004 The International Association for Biologicals. Published by Elsevier Ltd. All rights reserved.
doi:10.1016/j.biologicals.2004.08.002

treated with gene therapy protocols [2]. The FDA guidelines recommend that retrovirus vector products be tested for the presence of RCR by inoculation and passage of the test sample with a permissive cell line for a minimum of 5 passages in order to amplify any potential RCR present, followed by subsequent testing with an appropriate indicator cell assay. The PG-4 S + L− focus-forming assay and the marker rescue assays have been routinely used for the detection of RCR [3–7]. However, these conventional cell-based assays are known to have several disadvantages: the assays take a long time (weeks), visual evaluation of the results requires skill and is labor intensive, and the limited dynamic range requires many dilutions. Therefore, there is need for a more sensitive and rapid quantitative detection method for RCR.

Polymerase chain reaction (PCR) is a highly sensitive method for the detection of viral genomes [8]. It has been reported that PCR assays were capable of detecting one or more copies of RCR provirus in 500,000 cells [9]. PCR-based assay for RCR is used for biosafety monitoring of transduced cells with retroviral vectors [10] and of patients receiving retroviral gene therapy [9,11].

Moreover, the recently developed fluorescence-based real-time quantitative reverse transcription-PCR (RT-PCR) assay allows precise quantification of RNA genomes. Since quantitative RT-PCR can be performed in a short time with a wide dynamic range and high throughput, it is expected to be particularly suitable for quantifying RCR in viral stocks with high sensitivity. However, the PCR-based assay detects not only infectious virus genomes. In previous studies, PCR-based assays detected viral DNA fragments derived from packaging cell lines contaminated into retrovirus vector supernatants and caused false-positive findings [12,13]. Therefore, when quantitative RT-PCR is used for RCR detection, some process is required to distinguish infectious RCR RNA and viral DNA fragments prior to the quantitative RT-PCR assay. Infection of RCR into a permissive cell line is suitable for this purpose, because infectious RCR selectively replicates in cells without replication of viral DNA fragments and retrovirus vectors.

In addition, if RCR could be concentrated when preparing the sample for quantitative RT-PCR, it is expected that the sensitivity of RCR genome detection could be improved. In a previous study, our group demonstrated that polyethyleneimine (PEI)-conjugated magnetic beads efficiently adsorbed many types of viruses, with the exception of some non-enveloped viruses, and this novel virus concentration method using PEI-beads enhanced the sensitivity of virus detection by both PCR and RT-PCR [14].

In the present study, we have established a novel RCR detection method based on infectivity RT-PCR. Infectivity RT-PCR is a hybrid method that attempts to combine the best features of infectivity assays and quantitative RT-PCR. Samples are allowed to amplify in cell culture, as in conventional assays. Replication-competent retrovirus is quantified by real-time quantitative RT-PCR rather than by counting focuses. In addition, we applied a novel virus concentration method using PEI-beads to concentrate RCR in culture supernatants before quantitative RT-PCR. We demonstrated that this novel method could detect RCR more sensitively and rapidly than the conventional culture assays.

2. Materials and methods

2.1. Virus and cells

Hybrid Moloney/amphotropic *Murine leukemia virus* (MLV) obtained from ATCC (Manassas, VA; VR-1450; virus titer: $6.9 \pm 2.0 \times 10^7$ infectious unit (iu)/ml) was used as the RCR Reference Material. This hybrid virus, which was established by both the FDA and ATCC as an MLV RCR Reference Material, consists of Moloney MLV with a substitution of the *env* coding region from the 4070A strain of amphotropic MLV (AMLV), and represents a typical recombinant virus that could be generated in a retroviral packaging cell line containing coding sequences for an AMLV *env* [2].

Mus dunni cells (CRL-2017) and cat fibroblast PG-4 (S + L−) cells (CRL-2032) were obtained from ATCC. NIH/3T3 cells (JCRB0615) were obtained from the Japanese Cancer Research Resource Bank (Tokyo, Japan). ΨCRIP-P131 cells (RCB1088) were obtained from the RIKEN Cell Bank (Tsukuba, Japan). *M. dunni* cells and PG-4 (S + L−) cells were maintained in McCoy's 5A medium with 10% fetal calf serum (FCS). NIH/3T3 cells and ΨCRIP-P131 cells were maintained in Dulbecco's modified Eagle's medium (DMEM) supplemented with 10% calf serum.

2.2. Preparation of recombinant retrovirus vector

The retrovirus vector plasmid pLEGFP-N1 (Clontech, Palo Alto, CA) contains the enhanced green fluorescent protein (EGFP) and neomycin resistance gene. ΨCRIP-P131 cells which contain the *gag/pol* gene of Moloney MLV and *env* gene of 4070A in different expression vectors were used as a high titer retrovirus vector-packaging cell line. ΨCRIP-P131 cells (1×10^6 cells) were transfected with pLEGFP-N1 (2 μg) by Effectene Transfection Reagent (Qiagen, Hilden, Germany). Two days after transfection, cells were trypsinized and replated. The next day, Geneticin (GIBCO-BRL, Grand Island, NY; final concentration 1 mg/ml) were added to each dish and cultured for an additional 2 weeks. Eighteen clones of neomycin-resistant cells were picked up, and a clone (ΨCRIP-LEGFP1) which showed the

highest EGFP expression when the NIH/3T3 cells were infected with the culture supernatants of cloned cells was used as a line of retrovirus vector-producing cells. For the preparation of retrovirus vector sample, ΨCRIP-LEGFP1 cells were cultured to subconfluence, the medium was replaced with fresh medium, and after 24 h of culture, the culture supernatants were collected as retrovirus vector samples (vector titer: 1×10^6 cfu/ml). Vector supernatants were stored at −80 °C until use.

2.3. RCR concentration by PEI-beads

PEI-beads were made by coupling of PEI (MW 70,000; Wako Pure Chemical Inc., Tokyo, Japan) with magnetic beads (IMMUTEX-MAG™; mean diameter: 0.8 μm; JSR Inc., Tokyo, Japan) by the 1-ethylene-3-(3-dimethylaminopropyl)carbodiimide coupling method as described previously [14]. RCR concentration using PEI-beads was done as follows: various dilutions of RCR solution were prepared from RCR Reference Material diluted with DMEM. Then 1 or 10 ml of each RCR dilution was incubated with 100 μl of PEI-beads for 10 min at room temperature. Then the complexes of virus and PEI-beads were trapped by a magnetic field (for 1 ml: Magnetic Trapper™, Toyobo Co., Tokyo, Japan; for 10 ml: Dynal MOC-1™, Dynal AS, Oslo, Norway). The virus genome was extracted from the PEI-beads adsorbed fraction (the whole volume) or unadsorbed supernatant (100 μl) with an SMI-TEST EX R&D Kit (Genome Science Laboratories, Fukushima, Japan). Extracted nucleic acids were dissolved in 50 μl of DNase/RNase-free distilled water, and 10 μl of this solution was used for the quantitative RT-PCR reaction.

2.4. Real-time quantitative RT-PCR

The real-time quantitative RT-PCR for RCR was monitored on an ABI PRISM 7000 Sequence Detection System (Applied Biosystems, Foster City, CA). The reaction was carried out in a 50 μl reaction mixture containing 10 μl of extracted sample, 1 μM each of the forward and reverse primer, 0.2 μM of TaqMan probe, and 25 μl of TaqMan One-Step RT-PCR Master Mix Reagents with 1.25 μl of 40× MultiScribe and RNase Inhibitor (Applied Biosystems). The reaction conditions were as follows: the viral RNA was reverse-transcribed into cDNA for 30 min at 48 °C, then heat-inactivated for 10 min at 95 °C; PCR was then performed for 50 cycles of 15 s at 95 °C and 1 min at 60 °C. Standard curves were generated from RCR RNA extracted from RCR Reference Material in each RT-PCR assay and validated using linear regression analysis. The RCR genomes were quantified in infectious units (iu). One infectious unit of RCR measured by quantitative RT-PCR means that the sample contains virus genome RNA equivalent to 1 iu of RCR Reference Material. The sequences of the primer pair and the probe used were as follows: forward primer (AMLVenv-1018F): 5′-GCG GTC GTG GGC ACT TAT A-3′; reverse primer (AMLVenv-1082R): 5′-TGT TGG GAA GTG GCC GTA C-3′; TaqMan probe (AMLVenv-1040TM): 5′-(FAM)-ATC ATT CCA CCG CTC CGG CCA-(TAMRA)-3′. These sequences were designed to detect the *env* gene of 4070A AMLV using Primer Express Ver 1.0 Software (Applied Biosystems). The amplified product is predicted to be 64 base pairs (bp) in length.

2.5. Amplification of RCR by culture cells

M. dunni cells were plated in 60-mm dishes at 2×10^5 cells/dish and cultured overnight. Culture medium was replaced with 1 ml of polybrene solution (16 μg/ml) as well as 1 ml of virus solution and incubated for 4 h at 37 °C. Cells were washed with 1 ml of medium 3 times and incubated with 5 ml of fresh culture medium. Culture supernatants were collected at the indicated days for RCR concentration using PEI-beads and detected by quantitative RT-PCR.

2.6. S + L− focus-forming assay

The PG-4 cells were plated in 6-well plates at a concentration of 2×10^5 cells/well and incubated at 37 °C in 5% CO_2 overnight. On the day of infection, the medium was discarded, 1 ml of DEAE-Dextran (20 μg/ml in medium) was added to each well, and the cells were incubated for 30 min at 37 °C. Then 1 ml of test sample was added to each well and the cells were incubated for 2 h at 37 °C. Finally, the samples were replaced with 2 ml of fresh culture medium and cultured at 37 °C in 5% CO_2. Foci of transformed cells were examined microscopically on day 3 and day 7.

3. Results

3.1. Detection of RCR RNA by real-time quantitative RT-PCR

We first established the detection method of RCR RNA by real-time quantitative RT-PCR. Serial log dilutions of RCR solution were prepared, and viral genome RNA extracted from 100 μl of each RCR solution was analyzed by TaqMan quantitative RT-PCR. Forward and reverse primers as well as the TaqMan probe used for the detection of RCR were designed to detect the AMLV *env* sequence that exists in the RCR genome but not in the retroviral vector sequence (Fig. 1). Fig. 2 shows the standard curve generated from an amplification plot of the quantitative RT-PCR assay for RCR. A linear relationship was observed between the threshold cycle (C_T, the PCR cycle at which the

fluorescence of amplification first exceeds baseline) and the log-transformed input retroviral RNA genomes. The linearity of the standard curve was obtained at a range of 10^{-1}–10^{6} iu of RCR in 100 μl of the sample with a correlation coefficient of 0.998. The standard curve was reproducible for repeated assay (data not shown). Since C_T could not be calculated from virus solutions having concentrations below 0.1 iu, the detection limit of the quantitative RT-PCR for RCR was 0.1 iu.

3.2. Concentration of RCR by PEI-beads

In order to detect very low titers of RCR in the culture supernatants of infected cells, we tried to concentrate retrovirus particles using PEI-beads. One and 10 ml of RCR solution (10^{-5} dilution of RCR in DMEM) were incubated with 100 μl of PEI-beads, and fractionated into the PEI-beads adsorbed fraction and the unadsorbed supernatant fraction. Viral genome RNA extracted from each fraction was applied to RT-PCR and analyzed by agarose gel electrophoresis. As shown in Fig. 3A, RCR *env* RNA was detected by RT-PCR from the PEI-beads adsorbed fraction but not from the unadsorbed supernatant, indicating that RCR was efficiently adsorbed in the PEI-beads. When the starting volume of virus solution used for concentration was increased from 1 to 10 ml, the amounts of RCR RNA obtained in the PEI-beads adsorbed fraction were increased without any change in the unadsorbed fraction. To analyze the concentration of virus with PEI-beads quantitatively, serial log dilutions of RCR solution were fractionated with PEI-beads, and the amounts of RCR RNA in the adsorbed fraction and the unadsorbed fraction were quantified by real-time RT-PCR (Table 1, Fig. 3B). When solutions containing low concentrations of RCR were applied to PEI-beads, all of the retrovirus particles in the viral solutions were efficiently collected in the PEI-beads fraction. On the other hand, when a solution containing high concentration of RCR was applied to the PEI-beads, unadsorbed

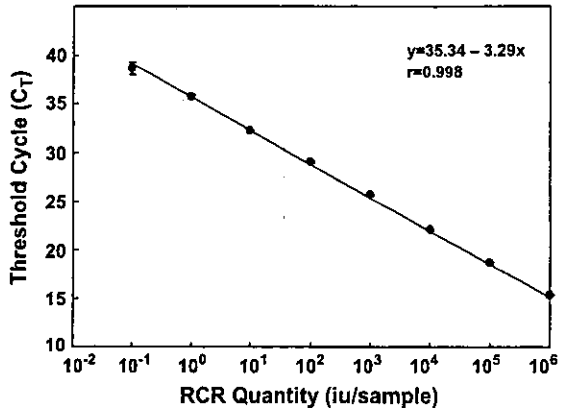

Fig. 2. Standard curve for the determination of RCR quantity generated from an amplification plot of real-time quantitative RT-PCR. Serial dilutions of RCR solution were analyzed by quantitative RT-PCR. A standard curve was generated from the amplification plot of RCR using real-time quantitative RT-PCR. The correlation coefficient is 0.998. Data are the mean ± S.D. ($n = 3$).

viruses were detected in the supernatant (Table 1). As a result, RCR treated with PEI-beads were maximally concentrated about 10-fold from 1 ml of virus solution and 100-fold from 10 ml of virus solution compared to direct extraction from 100 μl of original virus solutions, and at the same time, the assay sensitivity was increased about 10- and 100-fold, respectively (Table 1, Fig. 3B). These results clearly demonstrated that PEI-beads efficiently adsorbed RCR, and that this novel virus concentration method is useful for improving the sensitivity and lowering the limits of RCR detection.

3.3. Amplification of RCR in cell culture for infectivity RT-PCR

For the screening of RCR in retrovirus vector products, it is necessary to detect very less amounts of RCR among large amounts of retrovirus vectors. In our preliminary study, however, viral *env* DNA sequences derived from a packaging cell line were used to

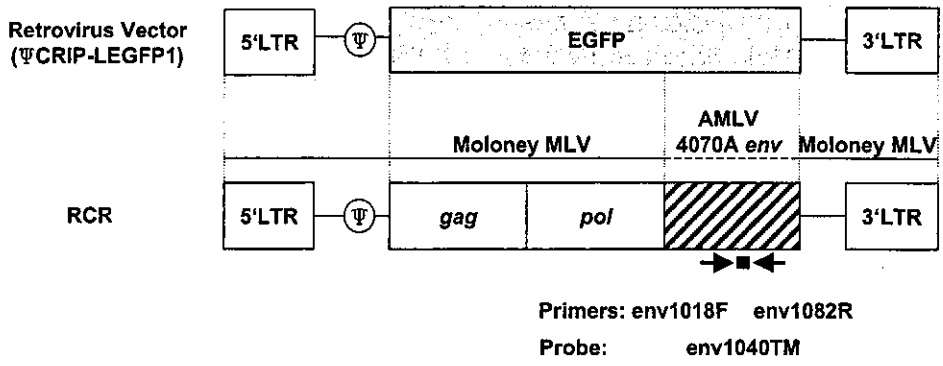

Fig. 1. Structure of RCR and retrovirus vector used in this study. The open bars represent Moloney MLV genome, the gray bar represents the expression cassette for the EGFP gene, and the striped bar represents the AMLV 4070A *env* gene. Black arrows and a small black square underneath the RCR genome indicate the location of the primers and a probe for RCR detection, respectively.

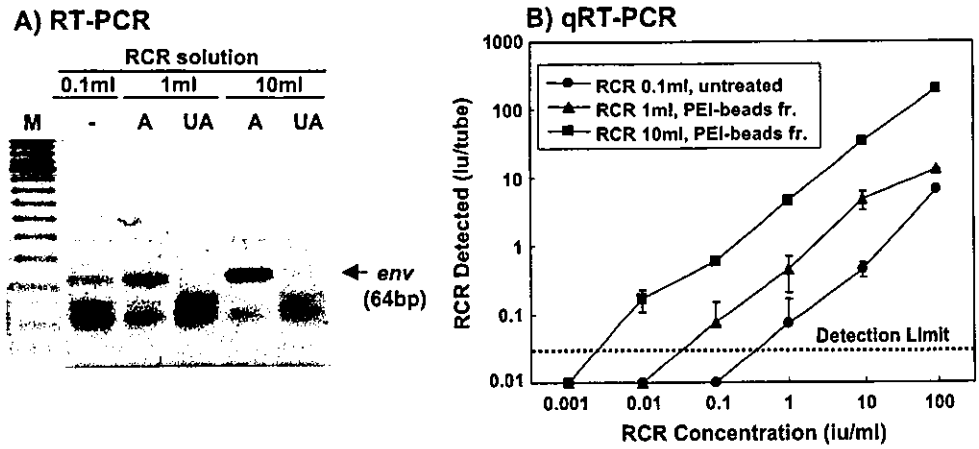

Fig. 3. Concentration of RCR by PEI-beads. (A) RCR solution (10^{-5} dilution) was fractionated with PEI-beads. Viral genome RNA extracted from the PEI-beads adsorbed fraction and unadsorbed supernatant were amplified with RT-PCR and analyzed by 5% agarose gel. M: 20 bp DNA ladder; –: untreated RCR solution; A: PEI-beads adsorbed fraction; UA: PEI-beads unadsorbed supernatant fraction. (B) One or 10 ml of serial dilutions of RCR solution was incubated with PEI-beads. Viral genome RNA extracted from the PEI-beads adsorbed fraction and untreated RCR solution was analyzed by real-time quantitative RT-PCR.

contaminate ΨCRIP-LEGFP1 retrovirus vector supernatants and detected using the same conditions used for the detection of RCR RNA (data not shown). Then, in order to detect only infectious RCR in retrovirus vector products by quantitative RT-PCR, we developed an infectivity RT-PCR. We first infected *M. dunni* cells with solutions containing various titers of RCR and cultured for several days. The replicated RCR in culture supernatants was then concentrated by PEI-beads and quantified by real-time RT-PCR.

Fig. 4 demonstrates the time course of the detection of RCR by infectivity RT-PCR. When *M. dunni* cells were infected with 10 or 100 iu of RCR, the viruses were linearly amplified from day 3 to day 7 (Fig. 4), and all 3 dishes had detectable amounts of virus even on day 2 (Table 2). When the cells were infected with 1 or 0.1 iu of RCR, amplification of RCR could be detected in more than one of the dishes after day 2 and day 5, respectively, though the level of amplification varied widely between the dishes (Table 2). RCR could not be amplified when the cells were infected with 0.01 iu of RCR. The same RCR solutions were also examined by direct S + L– assay using PG-4 cells (Table 2). We could not detect any focuses after 3 days of infection. On day 7, only when cells were infected with 100 iu of RCR, focuses were observed in 100% of wells. However, infection with 10 or 1 iu of RCR induced focus formation in only 1/2 or 1/6 of infected wells, respectively. These results demonstrated that infectivity RT-PCR was able to detect RCR more rapidly and 10- to 100-fold more sensitively than conventional S + L– assay.

3.4. Detection of RCR in retrovirus vector supernatant by infectivity RT-PCR

Finally, various amounts of RCR spiked in 10^6 cfu of retrovirus vector supernatant were examined by infectivity RT-PCR with RCR concentration by PEI-beads

Table 1
Quantitative analysis of RCR concentration using PEI-beads

RCR dilution	RCR quantity (iu/sample)				
	RCR 0.1 ml	RCR 1 ml		RCR 10 ml	
	Untreated	Adsorbed fr.	Unadsorbed fr. (0.1 ml)	Adsorbed fr.	Unadsorbed fr. (0.1 ml)
10^{-1}	2.0×10^6	4.0×10^6	4.9×10^1	6.3×10^6	6.3×10^7
10^{-2}	9.6×10^4	1.4×10^6	–	3.8×10^6	4.4×10^3
10^{-3}	3.7×10^3	3.4×10^4	–	7.2×10^5	1.5×10^0
10^{-4}	4.8×10^2	3.3×10^3	–	6.6×10^4	–
10^{-5}	2.4×10^1	1.2×10^2	–	2.6×10^3	–
10^{-6}	2.1×10^0	6.9×10^0	–	1.2×10^2	–
10^{-7}	–	3.8×10^{-1}	–	1.0×10^1	–
10^{-8}	–	–	–	5.0×10^{-1}	–
10^{-9}	–	–	–	–	–

Serial log dilutions of RCR solution (RCR Reference Material; original concentration: 6.9×10^7 iu/ml) were fractionated with PEI-beads. The amounts of RCR RNA extracted from the PEI-beads adsorbed fraction and unadsorbed fraction were quantified by real-time RT-PCR. –: Under detection limit.

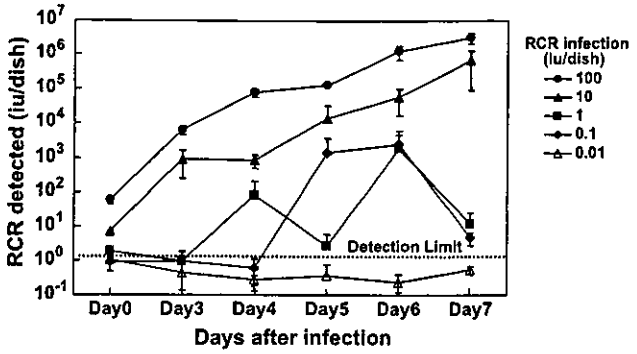

Fig. 4. RCR growth curve in *M. dunni* cells. *M. dunni* cells were infected with serial log dilutions of RCR solution. Culture supernatants were harvested at the indicated time, and RCR was concentrated by PEI-beads. Viral genome RNA was extracted from PEI-beads and the amount of RCR was determined by real-time quantitative RT-PCR. Data are the mean ± S.D. ($n = 3$).

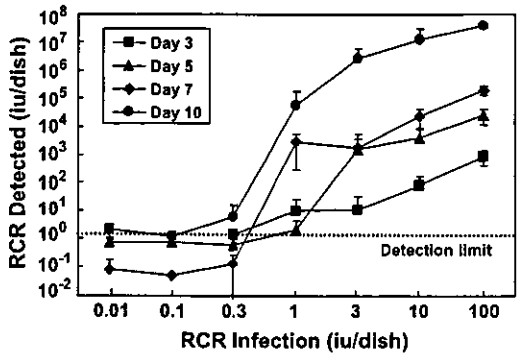

Fig. 5. Detection of RCR spiked in retrovirus vector supernatant by infectivity RT-PCR. *M. dunni* cells were infected with serial dilutions of RCR solution in 10^6 cfu/ml of ΨCRIP-LEGFP1 retrovirus vector supernatant. Cell culture supernatants of infected cells were harvested on day 3, 5, 7 and 10, and then RCR was concentrated by PEI-beads. The amount of RCR genome RNA extracted from the PEI-beads adsorbed fraction was determined by real-time quantitative RT-PCR. Data are the mean ± S.D. ($n = 5$).

(Fig. 5, Table 3). The amount of RCR was evaluated on 3, 5, 7, and 10 days after infection. Infectivity RT-PCR was able to detect 1 iu of RCR on day 3, and 0.3 iu of RCR on day 10 (Fig. 5). The detection ratio of 100% could be achieved for 10 iu on day 3 and 3 iu on day 5. We could not detect any *env* DNA from the culture supernatant of *M. dunni* cells after infection and cultivation of retrovirus vector supernatant (data not shown). When the same RCR samples were evaluated by direct S + L− assay, we could not detect any focuses on day 3, and focuses could be detected at 1 iu on day 7, although 100 iu was required for 100% detection (Table 3). Therefore, it is demonstrated that infectivity RT-PCR improved the level of sensitivity for the detection of RCR in retrovirus vector products 3- to 10-fold and shortened the assay period compared with the conventional S + L− assay.

4. Discussion

In the present study, we have developed a novel RCR detection method based on an infectivity RT-PCR and a virus concentration method using PEI-beads. Real-time quantitative RT-PCR is a suitable alternative to conventional RCR detection by infectivity assays because it is not only a quantitative but also a more sensitive method. However, viral *env* DNA derived from packaging cells was also detected in retrovirus vector supernatants used in this study under the same conditions used to detect RCR RNA (data not shown). Although RCR spiked in retrovirus vector supernatants was concentrated with PEI-beads, *env* DNA was also detected in the PEI-beads adsorbed fraction (data not shown). The mechanism of virus-adsorption by PEI-beads remains unclear, but it is hypothesized that the positive charge field of the PEI molecule might tightly interact with the negative charge of surface lipids or negatively charged proteins on viruses [14]. It is possible that PEI-beads adsorbed RCR particles as well as negatively charged DNA fragments. Therefore, to detect only infectious RCR by quantitative RT-PCR, infection and replication of virus in permissive cells is inevitable. The method of amplifying a virus in a permissive cell line, as used in infectivity RT-PCR, is also a common method to increase the assay sensitivity for virus detection, and is often used before conventional indicator cell

Table 2
Comparison of sensitivity of RCR detection by direct S + L− assay and infectivity RT-PCR

RCR infection (iu/dish)	Direct S + L− assay		Infectivity RT-PCR					
	Day 3	Day 7	Day 2	Day 3	Day 4	Day 5	Day 6	Day 7
100	− (0/6)	+ (6/6)	+ (3/3)	+ (3/3)	+ (3/3)	+ (3/3)	+ (3/3)	+ (3/3)
10	− (0/6)	± (3/6)	+ (3/3)	+ (3/3)	+ (3/3)	+ (3/3)	+ (3/3)	+ (3/3)
1	− (0/6)	± (1/6)	± (1/3)	± (1/3)	± (1/3)	± (1/3)	+ (3/3)	± (2/3)
0.1	− (0/6)	− (0/6)	− (0/3)	− (0/3)	− (0/3)	+ (3/3)	± (2/3)	+ (3/3)
0.01	− (0/6)	− (0/6)	− (0/3)	− (0/3)	− (0/3)	− (0/3)	− (0/3)	− (0/3)

Serial log dilutions of RCR solution were evaluated by direct PG-4 (S + L−) assay or infectivity RT-PCR conducted in conjunction with virus concentration using PEI-beads. Data are presented as positive assays (dishes or wells) over the total number of assays performed. +: All the dishes or wells were positive for RCR; ±: at least one dish or well was positive; −: none of the replicates were positive.

Table 3
Comparison of direct S + L− assay and infectivity RT-PCR on RCR detection spiked in retrovirus vector supernatant

RCR infection (iu/dish)	Direct S + L− assay		Infectivity RT-PCR			
	Day 3	Day 7	Day 3	Day 5	Day 7	Day 10
100	− (0/5)	+ (5/5)	+ (5/5)	+ (5/5)	+ (5/5)	+ (5/5)
10	− (0/5)	± (4/5)	+ (5/5)	+ (5/5)	+ (5/5)	+ (5/5)
3	− (0/5)	± (2/5)	± (1/5)	+ (5/5)	± (3/5)	+ (5/5)
1	− (0/5)	± (1/5)	± (2/5)	± (2/5)	± (4/5)	± (3/5)
0.3	− (0/5)	− (0/5)	− (0/5)	− (0/5)	− (0/5)	± (1/5)
0.1	− (0/5)	− (0/5)	− (0/5)	− (0/5)	− (0/5)	− (0/5)
0.01	− (0/5)	− (0/5)	− (0/5)	− (0/5)	− (0/5)	− (0/5)

Serial dilutions of RCR in 10^6 cfu/ml of ΨCRIP-LEGFP1 retrovirus vector supernatant were evaluated by direct PG-4 (S + L−) assay or infectivity RT-PCR conducted in conjunction with viral concentration using PEI-beads. Data are presented as positive assays (dishes or wells) over the total number of assays performed. +: All the dishes or wells were positive for RCR; ±: at least one dish or well was positive; −: none of the replicates were positive.

assays. In infectivity RT-PCR, the indicator cell assay was replaced by quantitative RT-PCR subsequent to the amplification of viruses.

Concentration of retrovirus particles is a simple method to increase the sensitivity of RCR detection. Several approaches to concentrate viruses have been tried in an attempt to enhance the sensitivity of virus genome detection [15–17]. Ultra-centrifugation is widely used for virus concentration, although it is associated with loss of infectivity of MLV [18]. Centrifugation at high-speeds for long duration has been used for concentration of retrovirus vectors [19,20], but this method is very time-consuming and not suitable for virus screening. Polyethylene-glycol (PEG) precipitation is a simple and easy method to concentrate several viruses, but the excess amount of PEG hampers the PCR reaction. In the present study, we have demonstrated that PEI-beads efficiently concentrated RCR in proportion to the volume of virus solution used for the assays. Virus concentration with PEI-beads is a simple and rapid method and is suitable for multiple sample preparation for quantitative RT-PCR.

By the combination of infectivity RT-PCR and virus concentration with PEI-beads, we have developed a novel RCR detection method. We demonstrated that 1 iu of RCR spiked in 10^6 cfu/ml of vector products could be detected within 3 days, and the sensitivity for viral detection was increased 3- to 10-fold compared with the direct S + L− assay. By this method, the presence of retroviral vector interfered with RCR detection [5] only slightly. As a result, this method can detect infectious RCR more rapidly and more sensitively and less labor intensive than conventional cell assays. However, the detection sensitivity was not additively improved as expected from the data of quantitative RT-PCR and virus concentration by PEI-beads. We consider that the limiting step of the detection of RCR by infectivity RT-PCR is the initial infection of the permissive cells with the virus, and thus it is difficult to improve the sensitivity after the replication step. In this case, improvement of the infection process may increase the detection sensitivity. We used polybrene for enhancing viral infectivity, as is done in conventional infectivity assays, but the effect was limited. It has been reported that spinoculation, in which RCR samples are inoculated under centrifugation, increased the sensitivity of RCR detection by the S + L− assay and marker rescue assays [6]. Alternatively, co-precipitation of retrovirus vector with calcium phosphate [21] or complexation with polybrene and chondroitin sulfate C [22] has been shown to increase the transduction efficiency. Utilizing these methods may be useful for increasing the infectivity sensitivity of RCR detection by infectivity RT-PCR.

The RCR detection method described here was designed to specifically detect infectious AMLV RCR in retrovirus vector products. The same strategy should be applied to RCRs other than AMLV by using primers and a probe designed to detect the specific RCR RNA. Furthermore, the infectivity (RT-) PCR strategy may be applicable to the detection of other replication-competent viruses. We have demonstrated that the infectivity PCR method was superior to the conventional cell culture/CPE method for detecting replication-competent adenovirus and useful for the detection of RCA in adenovirus vector products [23].

In conclusion, infectivity RT-PCR conducted in conjunction with virus concentration using PEI-beads can detect infectious RCR more sensitively and rapidly than the conventional infectivity assay. This novel method would be useful for detecting RCR in retrovirus vector products.

Acknowledgements

This work was supported by grants from the Ministry of Health, Labor and Welfare of Japan and from the Ministry of Education, Culture, Sports, Science and Technology of Japan.

References

[1] Donahue RE, Kessler SW, Bodine D, McDonagh K, Dunbar C, Goodman S, et al. Helper virus induced T cell lymphoma in nonhuman primates after retroviral mediated gene transfer. J Exp Med 1992;176:1125–35.

[2] Supplemental guidance on testing for replication-competent retrovirus in retroviral vector-based gene therapy products and during follow-up of patients in clinical trials using retroviral vectors. Hum Gene Ther 2001;12:315–20.

[3] Bassin RH, Ruscetti S, Ali I, Haapala DK, Rein A. Normal DBA/2 mouse cells synthesize a glycoprotein which interferes with MCF virus infection. Virology 1982;123:139–51.

[4] Markowitz D, Goff S, Bank A. Construction and use of a safe and efficient amphotropic packaging cell line. Virology 1988;167: 400–6.

[5] Printz M, Reynolds J, Mento SJ, Jolly D, Kowal K, Sajjadi N. Recombinant retroviral vector interferes with the detection of amphotropic replication competent retrovirus in standard culture assays. Gene Ther 1995;2:143–50.

[6] Forestell SP, Dando JS, Bohnlein E, Rigg RJ. Improved detection of replication-competent retrovirus. J Virol Methods 1996;60: 171–8.

[7] Miller AD, Bonham L, Alfano J, Kiem HP, Reynolds T, Wolgamot G. A novel murine retrovirus identified during testing for helper virus in human gene transfer trials. J Virol 1996;70: 1804–9.

[8] Saiki RK, Gelfand DH, Stoffel S, Scharf SJ, Higuchi R, Horn GT, et al. Primer-directed enzymatic amplification of DNA with a thermostable DNA polymerase. Science 1988;239:487–91.

[9] Long Z, Lu P, Grooms T, Mychkovsky I, Westley T, Fitzgerald T, et al. Molecular evaluation of biopsy and autopsy specimens from patients receiving in vivo retroviral gene therapy. Hum Gene Ther 1999;10:733–40.

[10] Morgan RA, Cornetta K, Anderson WF. Applications of the polymerase chain reaction in retroviral-mediated gene transfer and the analysis of gene-marked human TIL cells. Hum Gene Ther 1990;1:135–49.

[11] Long Z, Li LP, Grooms T, Lockey C, Nader K, Mychkovsky I, et al. Biosafety monitoring of patients receiving intracerebral injections of murine retroviral vector producer cells. Hum Gene Ther 1998;9:1165–72.

[12] Chen J, Reeves L, Sanburn N, Croop J, Williams DA, Cornetta K. Packaging cell line DNA contamination of vector supernatants: implication for laboratory and clinical research. Virology 2001;282:186–97.

[13] Chen J, Reeves L, Cornetta K. Safety testing for replication-competent retrovirus associated with gibbon ape leukemia virus-pseudotyped retroviral vectors. Hum Gene Ther 2001;12:61–70.

[14] Satoh K, Iwata A, Murata M, Hikata M, Hayakawa T, Yamaguchi T. Virus concentration using polyethyleneimine-conjugated magnetic beads for improving the sensitivity of nucleic acid amplification tests. J Virol Methods 2003;114:11–9.

[15] Sanyal D, Kudesia G, Corbitt G. Comparison of ultracentrifugation and polyethylene glycol precipitation for concentration of hepatitis B virus (HBV) DNA for molecular hybridisation tests and the relationship of HBV-DNA to HBe antigen and anti-HBe status. J Med Microbiol 1991;35:291–3.

[16] Kittigul L, Khamoun P, Sujirarat D, Utrarachkij F, Chitpirom K, Chaichantanakit N, et al. An improved method for concentrating rotavirus from water samples. Mem Inst Oswaldo Cruz 2001;96: 815–21.

[17] Li JW, Wang XW, Rui QY, Song N, Zhang FG, Ou YC, et al. A new and simple method for concentration of enteric viruses from water. J Virol Methods 1998;74:99–108.

[18] Kamps CA, Lin YC, Wong PK. Oligomerization and transport of the envelope protein of Moloney murine leukemia virus-TB and of ts1, a neurovirulent temperature-sensitive mutant of Mo-MuLV-TB. Virology 1991;184:687–94.

[19] Bowles NE, Eisensmith RC, Mohuiddin R, Pyron M, Woo SL. A simple and efficient method for the concentration and purification of recombinant retrovirus for increased hepatocyte transduction in vivo. Hum Gene Ther 1996;7:1735–42.

[20] Yang J, Friedman MS, Bian H, Crofford LJ, Roessler B, McDonagh KT. Highly efficient genetic transduction of primary human synoviocytes with concentrated retroviral supernatant. Arthritis Res 2002;4:215–9.

[21] Morling FJ, Russell SJ. Enhanced transduction efficiency of retroviral vectors coprecipitated with calcium phosphate. Gene Ther 1995;2:504–8.

[22] Le Doux JM, Landazuri N, Yarmush ML, Morgan JR. Complexation of retrovirus with cationic and anionic polymers increases the efficiency of gene transfer. Hum Gene Ther 2001;12: 1611–21.

[23] Ishii-Watabe A, Uchida E, Iwata A, Nagata R, Satoh K, Fan K, et al. Detection of replication-competent adenovirus spiked into recombinant adenovirus vector products by infectivity-PCR. Mol Ther 2003;8:1009–16.

日本再生医療学会雑誌

再生医療

Regenerative Medicine

2004

5

Vol.3 No.2

別刷

メディカルレビュー社

〒541-0046 大阪市中央区平野町1-7-3 吉田ビル TEL 06-6223-1468
〒113-0034 東京都文京区湯島3-19-11イトーピア湯島ビル TEL 03-3835-3041

Novel mechanism of tumorigenesis: Increased transforming growth factor-β1 suppresses the expression of connexin 43 in BALB/cJ mice after implantation of poly-L-lactic acid

Saifuddin Ahmed, Toshie Tsuchiya
Division of Medical Devices, National Institute of Health Sciences, 1-18-1, Kamiyoga, Setagaya ku, Tokyo 158-8501, Japan

Received 15 December 2003; revised 24 March 2004; accepted 6 April 2004
Published online 4 June 2004 in Wiley InterScience (www.interscience.wiley.com). DOI: 10.1002/jbm.a.30090

Abstract: Poly-L-lactic acid (PLLA) is a widely used promising material for surgical implants such as tissue-engineered scaffolds. In this study, we aimed to determine the *in vivo* effect of PLLA plates on the cellular function of subcutaneous tissue in the two mouse strains, BALB/cJ and SJL/J, higher and lower tumorigenic strains, respectively. Gap-junctional intercellular communication (GJIC) and the expression of connexin 43 (Cx43) protein were significantly suppressed, whereas the secretion of transforming growth factor-β1 (TGF-β1) level was significantly increased in PLLA-implanted BALB/cJ mice compared with BALB/cJ controls. However, no significant difference in TGF-β1 secretion was observed between the SJL/J-implanted and SJL/J control mice. We found for the first time that a significant difference was observed between the two strains; thus, the PLLA increased the secretion of TGF-β1 and suppressed the mRNA expression of Cx43 at the earlier stage after implantation into the higher-tumorigenic strain, BALB/cJ mice. This novel mechanism might have a vital role in the inhibition of GJIC and promote the tumorigenesis in BALB/cJ mice. © 2004 Wiley Periodicals, Inc. J Biomed Mater Res 70A: 335–340, 2004

Key words: poly-L-lactic acid; gap-junctional intercellular communication (GJIC); connexin 43; transforming growth factor (TGF)-β; tumorigenesis

INTRODUCTION

The implantation of a biomaterial always induces a host inflammatory response. The extent and resolution of these responses have a vital role in determining the long-term success of implanted medical devices.[1–3] Poly-L-lactic acid (PLLA) is a widely used material for surgical implants and clinically as a bioabsorbable suture material.[4,5] Polyurethanes (PUs) have also been used for implant applications because of their useful elastomeric properties and high tensile strength, lubricity, and good abrasion resistance. Some adverse effects of the biomaterials, such as PLLA and PUs, have been reported in animal experiments. Long-term implants of PLLA produced tumorigenicity in rats.[6] Different kinds of PUs induced various tumor incidences in rats.[7] All tumors have been generally viewed as the outcome of disruption of the homeostatic regulation of the cellular ability to respond to extracellular signals, which trigger intracellular signal transduction abnormalities.[8] During the evolutionary transition from the single-cell organism to the multicellular organism, many genes appeared to accompany these cellular functions. One of these genes was the gene coding for a membrane-associated protein channel (the gap junction).[9] Gap-junctional intercellular communications (GJIC) are transmembrane channels that allow the cell–cell transfer of small molecules and are composed of protein subunits known as connexin; at least 19 connexins exist and they are expressed in a cell- and development-specific manner.[10,11] GJIC also has an important role in the maintenance of cell homeostasis and in the control of cell growth.[12] So, the loss of GJIC has been considered to cause abnormal development and tumor formation.[13–15] Several tumor promoters have been shown to restrict GJIC by phosphorylation of connexin proteins, such as connexin 43 (Cx43), which is an essential

Correspondence to: T. Tsuchiya; e-mail: tsuchiya@nihs.go.jp
Contract grant sponsor: Health and Labour Sciences Research Grants
Contract grant sponsor: Research on Advanced Medical Technology, Ministry of Health, Labour and Welfare
Contract grant sponsor: Japan Health Sciences Foundation

protein to form the gap-junction channel.[16,17] We have hypothesized that the different tumorigenic potentials of PLLA and PUs are caused mainly by the different tumor-promoting activities of these biomaterials. Therefore, we investigated the effects of PLLA on the subcutaneous tissue between the two strains of female mice, BALB/cJ and SJL/J.

MATERIALS AND METHODS

Animals

Five-week-old female BALB/cJ and SJL/J mice were purchased from Charles River (Japan) and maintained in the animal center according to the animal welfare National Institute of Health Sciences guidance. All mice were fed with standard pellet diets and water *ad libitum*, before and after the implantation.

Implantation of PLLA

PLLA was obtained from Shimadzu Co. Ltd. as uniform plates. Implants (size: 20 × 10 × 1 mm, weight-average molecular weight 200,000) were sterilized using ethylene oxide gas before use. Sodium pentobarbital (4 mg/kg) was intraperitoneally administered to the mice. The dorsal skin was shaved and scrubbed with 70% alcohol. Using an aseptic technique, an incision of approximately 2 cm was made; away from the incision, a subcutaneous pocket was formed by blunt dissection, and one piece of PLLA was placed in the pocket. The incision was closed with silk threads. In both strains, controls were obtained by sham operation and subsequent subcutaneous pocket formation. After surgery, the mice were housed in individual cages. After 30 days, mice from the implanted group were sacrificed, implanted materials were excised out, and subcutaneous tissues from the adjacent sites were collected for culture. At the same time, subcutaneous tissues were removed from the sites in the sham-operated controls that correlated with the implant sites.

Cell culture of subcutaneous tissues

The subcutaneous tissues were maintained in minimum essential medium supplemented with 10% fetal bovine serum in a 5% CO_2 atmosphere at 37°C.

Scrape-loading and dye transfer (SLDT) assay

SLDT technique was performed by the method of El-Fouly et al.[18] Confluent monolayer cells in 35-mm culture dishes were used. After rinsing with Ca^{2+} Mg^{2+} phosphate-buffered saline [PBS (+)], cell dishes were loaded with 0.1% Lucifer Yellow (Molecular Probes, Eugene, OR) in PBS (+) solution and were scraped immediately with a sharp blade. After incubation for 5 min at 37°C, cells were washed three times with PBS (+) and the extent of dye transfer was monitored using a fluorescence microscope, equipped with a type UFX-DXII CCD camera and super high-pressure mercury lamp power supply (Nikon, Tokyo, Japan).

Western blot analysis

When cells grew confluently in 60-mm tissue culture dishes, all cells were lysed directly in 100 μL of 2% sodium dodecyl sulfate (SDS) gel loading buffer (50 m*M* Tris-HCl, pH 6.8, 100 m*M* 2-mercaptoethanol, 2% SDS, 0.1% bromophenol blue, 10% glycerol). The protein concentration of the cleared lysate was measured using the microplate BCA (bicinchoninic acid) protein assay (Pierce, Rockford, IL). Equivalent protein samples were analyzed by 7.5% SDS–polyacrylamide gel electrophoresis. The proteins were transferred to Hybond-ECL nitrocellulose membranes (Amersham Pharmacia Biotech UK Ltd., Buckinghamshire, UK). Cx43 protein was detected by anti-Cx43 polyclonal antibodies (ZYMED Laboratories, Inc., San Francisco, CA). The membrane was soaked with Block Ace (Yukijirusi Nyugyo, Sappro, Japan), reacted with the anti-Cx43 polyclonal antibodies for 1 h, and after washes with PBS containing 0.1% Tween20, reacted with the secondary anti-rabbit immunoglobulin G antibody conjugated with horseradish peroxidase for 1 h. After several washes with PBS–Tween20, the membrane was detected with the ECL detection system (Amersham Pharmacia Biotech UK Ltd.).

Reverse transcriptase polymerase chain reaction (RT-PCR)

Cx43 mRNA expression was verified by RT-PCR. Total cellular RNA was isolated from cultured cells in Trizol reagent (Life Technologies, Inc., Frederick, MD) following the manufacturer's instructions. The concentration of total RNA was determined using a UV spectrophotometer (Gene Quant; Pharmacia Biotech, Piscataway, NJ). cDNA was synthesized from 1 μg of total RNA by RT using the First-Strand cDNA synthesis kit (Amersham Pharmacia Biotech, Uppsala, Sweden). Amplification was performed in a volume of 25 μL containing 1 μL of cDNA, 10 pmol of each primer, 0.625 unit of *Taq* polymerase (Promega, Madison, WI) and 0.2 m*M* of each deoxynucleotide triphosphate. The sequence of the primer pairs were as follows: forward 5′-ACAGTCTGCCTTTCGCTGTAAC-3′ and reverse 5′-GTAAGGATCGCTTCTTCCCTTC-3′. The PCR cycle was as follows: initial denaturation at 94°C for 5 min, followed by 25 cycles of 94°C for 1 min, 60°C for 1 min, and 72°C for 1 min, with final extension at 72°C for 7 min. The amplified product was separated on 1.5% agarose gel and visualized with SYBR Green I (BioWhittaker Molecular Applications, Rockland, ME). For relative quantitation, the signal intensity of each lane was standardized to that of a housekeeping gene,

GAPDH. To amplify this gene, the following primer pairs were used: forward 5′-CCCATCACCATCTTCCAGGAGC-GAGA-3′ and reverse 5′-TGGCCAAGGTCATCCATGA-CAACTTTGG-3′.

Enzyme-linked immunosorbent assay (ELISA)

Cells were seeded onto 60-mm dishes. The conditioned medium was collected and obtained after the centrifugation at 1000 rpm for 2 min. The transforming growth factor (TGF)-β levels of the media were measured with commercially available ELISA kits (R&D Systems Inc., Minneapolis, MN).

Cytokine treatment

Here, we used sham-operated BALB/cJ mice cells as a control. One hundred thousand cells were seeded onto 35-mm tissue culture dishes and cultured. After 4 h seeding in a 5% CO_2 atmosphere at 37°C, cells were treated with TGF-β1 (0, 2, and 10 ng/mL). Thereafter, SLDT and RT-PCR were performed. Purified human TGF-β1 was purchased from R&D Systems.

Statistical analysis

Student *t* test was used to compare the implanted samples with the controls. Statistical significance was accepted at $p < 0.05$. Values were presented as the mean ± standard deviation.

RESULTS AND DISCUSSION

There are many known tumorigenesis-inducing factors. It was reported that many plastics induce malignant tumors when implanted subcutaneously into rats and mice.[19–22] PLLA shows slow degradation, and therefore has been applied as a biomaterial for surgical devices such as bone plates, pins, and screws. It was reported in different studies that polyetherurethane, polyethylene, and PLLA produced tumors in rats.[6,7,23–25] In our study, tumors were induced by PLLA plates in BALB/cJ mice at 100% incidence but not in SJL/J mice at the surrounding tissues of PLLA plates during a 10-month *in vivo* study. To understand the mechanisms of tumorigenesis induced by PLLA, we focused on the inhibitory effects on GJIC at the early stage of tumorigenesis. To assess functional GJIC, the SLDT assay was performed. Brand et al.[26] reported that BALB/cJ mice are a higher and SJL/J mice are a lower tumorigenic strain. Our present results showed that the GJIC was significantly inhibited in 1-month PLLA-implanted BALB/cJ mice cells compared with BALB/cJ controls (Fig. 1). In contrast, no significant difference was observed between the 1-month PLLA-implanted SJL/J mice and SJL/J controls (Fig. 1). The data also revealed that the dye migration was higher in control BALB/cJ mice than control SJL/J mice (Fig. 1). High responder to the tumorigenicity may be classified as animals that are easily suppressed in both GJIC function and the connexins expression. This perturbed gap junction is likely to have a major role in the PLLA-induced tumorigenesis. Gap junctions are also regulated by the posttranslational phosphorylation of the carboxy-terminal tail region on the connexin molecule. Phosphorylation of connexin molecules is closely related with the inhibition of GJIC.[27,28] Phosphorylation has been involved in controlling a broad variety of connexin processes that include trafficking, gathering/nongathering, degradation, and also the gating of gap channels. It was also reported that communication-deficient cells did not express the Cx43–biphosphorylated (P_2) isoform but cells with low gap-junction permeability showed detectable amounts of the Cx43–monophosphorylated (P_1) isoform.[16] To survey the cause, we examined the mRNA and protein expression of the Cx43 gene. Here, mRNA expression was suppressed in PLLA-implanted BALB/cJ mice compared with BALB/cJ controls [Fig. 2(A)]. No significant difference was observed between the PLLA-implanted SJL/J mice and SJL/J controls [Fig. 2(B)]. We also found that the total level of protein expression such as unphos-

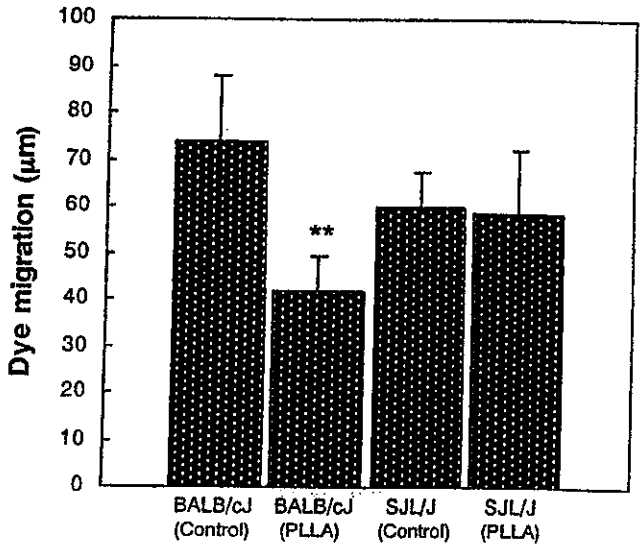

Figure 1. Statistical analysis of the SLDT assay. In both the implanted and sham-operated controls, three mice of each strain were sacrificed after 30 days. Results shown are representative of two independent experiments. GJIC was significantly inhibited in PLLA-implanted BALB/cJ mice cells compared with BALB/cJ controls. $^{**}p < 0.01$.

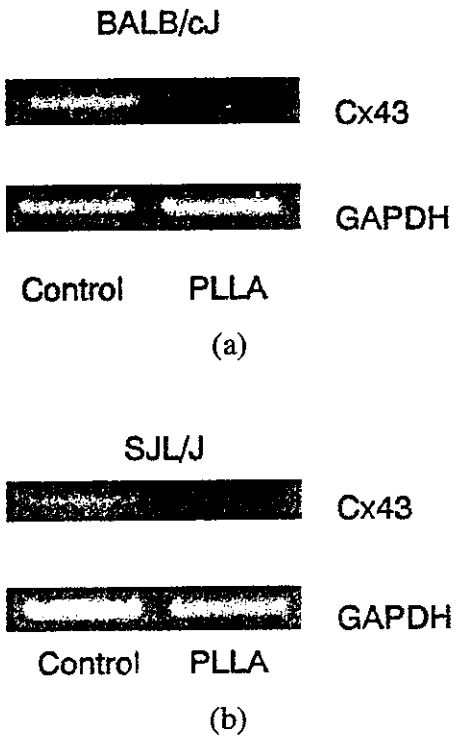

Figure 2. mRNA expression of Cx43 by RT-PCR analysis. In both the implanted and sham-operated controls, three mice of each strain were sacrificed after 30 days. Results shown are representative of two independent experiments. SYBR Green I stained PCR products after agarose gel electrophoresis showed that (A) mRNA expression was suppressed in PLLA-implanted BALB/cJ mice compared with BALB/cJ controls, and (B) no significant difference was observed between the PLLA-implanted SJL/J mice and SJL/J controls.

phorylated (P_0), P_1, and P_2 levels were significantly decreased in PLLA-implanted BALB/cJ mice compared with the control (Fig. 3). Asamoto et al.[29] reported that tumorigenicity was enhanced when the expression of Cx43 protein was suppressed by the anti-sense RNA of Cx43. A similar tendency was also observed in our study where the protein expression might be inhibited via down-regulation of the mRNA level. The genetic alteration and posttranslational

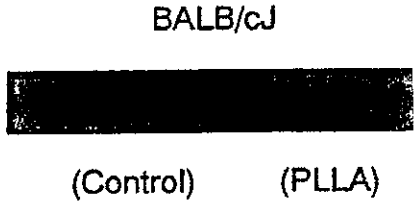

Figure 3. Protein expression of Cx43 by Western blot analysis. In both the implanted and sham-operated controls, three mice of each strain were sacrificed after 30 days. Results shown are representative of two independent experiments. Total level of protein expression such P_0, P_1, and P_2 levels were significantly decreased in PLLA-implanted BALB/cJ mice compared with the controls.

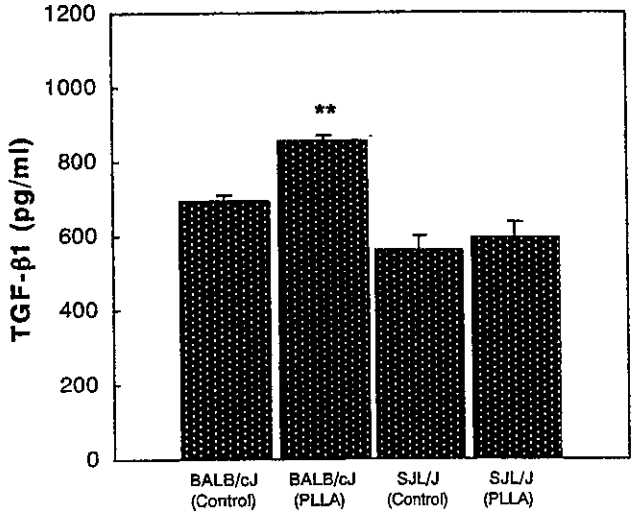

Figure 4. Statistical analysis of TGF-β1 cytokine assay by ELISA. In both the implanted and sham-operated controls, three mice of each strain were sacrificed after 30 days. Results shown are representative of two independent experiments. Secretion of the TGF-β1 level was significantly increased in PLLA-implanted BALB/cJ mice compared with BALB/cJ controls. $^{**}p < 0.01$.

modification in the Cx43 protein was shown to be involved in impaired GJIC and could be associated with tumorigenesis. Therefore, it is suggested that the inhibitory effect of PLLA on GJIC might be caused by the alteration in the Cx43 protein, causing enhancement of tumorigenesis. Moreover, Moorby and Patel[30] reported a direct action of the Cx43 protein on cell growth that was mediated via the cytoplasmic carboxyl domain.

Because TGF-β1 inhibits GJIC by decreasing the phosphorylated form of Cx43[31] and the phosphorylation of Cx43 has been implicated in gap-junction assembly and gating events,[16,27,32] we hypothesized that TGF-β1 might have an important role on PLLA-implanted BALB/cJ mice. Figure 4 clearly demonstrates that the secretion of the TGF-β1 level was significantly increased in PLLA-implanted BALB/cJ subcutaneous tissue in comparison with those from BALB/cJ control mice. No significant difference was found in the secretion of TGF-β1 between the SJL/J implanted and SJL/J control mice. TGF-β2 and TGF-β3 cytokine assay revealed no significant difference in TGF-β2 secretion and TGF-β3 was below the detection level (data not shown). So we performed an *in vitro* study, which showed that the intercellular communication and the mRNA expression of Cx43 were significantly suppressed in BALB/cJ control cells when treated with TGF-β1 [Fig. 5(A,B)].

In conclusion, we suggest that increased secretion of TGF-β1 (Fig. 4) suppressed expression of the gap-junctional protein Cx43 (Fig. 3) at the earlier stage after implantation of PLLA in BALB/cJ mice, resulting in

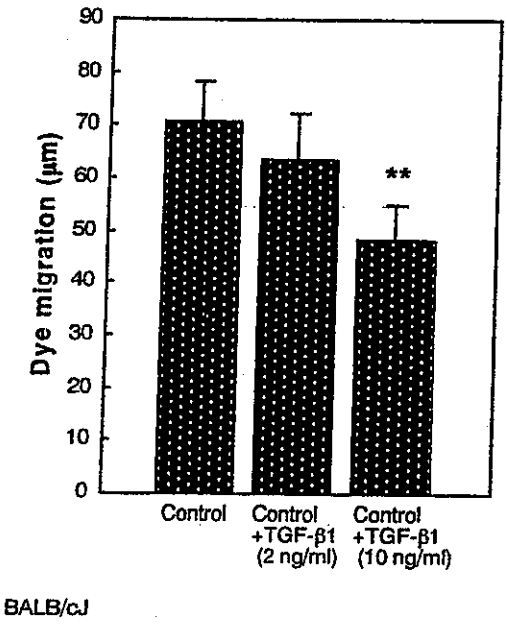

(a)

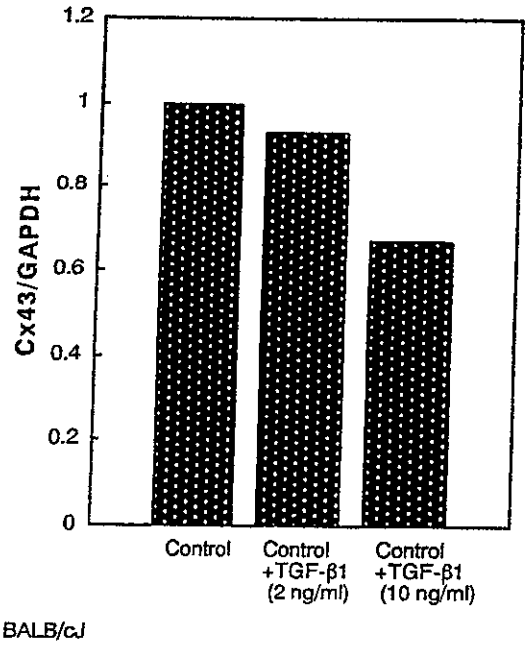

(b)

Figure 5. (A) SLDT assay. (B) National Institutes of Health image analysis quantitation of RT-PCR bands. In both figures, BALB/cJ control cells were treated with 2 and 10 ng/mL TGF-β1. GJIC was significantly inhibited and mRNA expression was significantly suppressed in BALB/cJ control cells treated with 10 ng/mL TGF-β1 compared with BALB/cJ controls. $^{**}p < 0.01$. Three dishes were used for one data point (bar) as one experiment. Results shown are representative of two independent experiments.

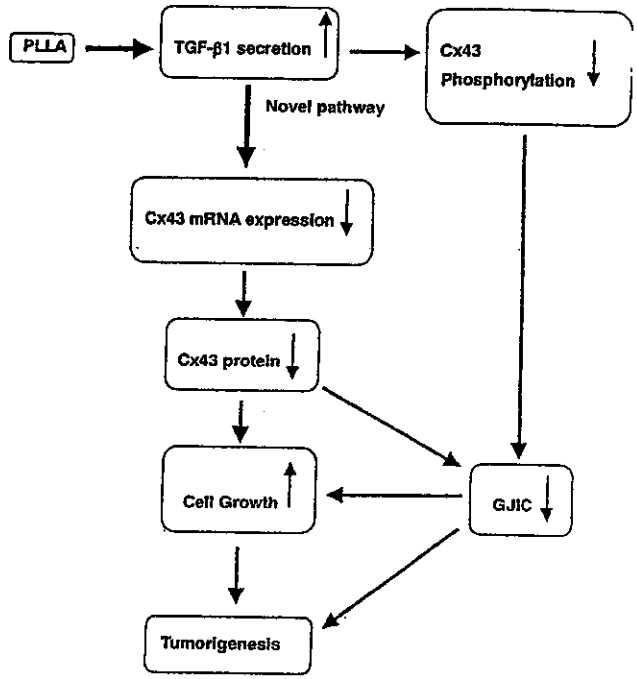

Figure 6. Schematic representation of the pathway of tumorigenesis induced by PLLA in BALB/cJ mice.

the suppression of the function of GJIC (Fig. 1) and at the same time, mRNA expression of Cx43 was suppressed in BALB/cJ mice (higher tumorigenic) but not in SJL/J mice (lower tumorigenic) [Fig. 2(A,B)]. TGF-β1 also suppressed the expression of mRNA of Cx43 and the function of GJIC in the BALB/cJ mouse cells *in vitro* [Fig. 5(A,B)]. These results indicated the novel mechanism of tumorigenesis induced by PLLA (Fig. 6).

References

1. Tang L, Eaton JW. Inflammatory responses to biomaterials. Am J Clin Pathol 1995;103:466–471.
2. Rames A, Williams DF. Immune response in biocompatibility. Biomaterials 1992;13:731–743.
3. Anderson JM. Mechanisms of inflammation and infection with implanted devices. Cardiovasc Pathol 1993;2:33s–41s.
4. Kulkarni RK, Pani KC, Neuman C, Leonard F. Polylactic acid for surgical implants. Arch Surg 1966;93:839–843.
5. Craig PH, Williams JA, Davis KW, Magoun AD, Levy AJ, Bogdansky S, Jones JP Jr. A biological comparison of polyglactin 910 and polyglycolic acid synthetic absorbable sutures. Surg Gynecol Obstet 1995;141:1–10.
6. Nakamura T, Shimizu Y, Okumura N, Matsui T, Hyon SH, Shimamoto T. Tumorigenicity of poly-L-lactide (PLLA) plates compared with medical-grade polyethylene. J Biomed Mater Res 1994;28:17–25.
7. Nakamura A, Kawasaki Y, Takada K, Aida Y, Kurokama Y, Kojima S, Shintani H, Matsui M, Nohmi T, Matsuoka A, Sofuni T, Kurihara M, Miyata N, Uchima T, Fujimaki M. Difference in tumor incidence and other tissue responses to polyetherurethanes and polydimethylsiloxane in long-term subcutaneous implantation into rats. J Biomed Mater Res 1992;26:631–650.

8. Trosko JE, Madhukar BV, Chang CC. Endogenous and exogenous modulation of gap junctional intercellular communication: toxicological and pharmacological implications. Life Sci 1993;53:1–19.
9. Trosko JE, Ruch RJ. Cell–cell communication in carcinogenesis. Front Biosci 1998;3:D208–236.
10. Eiberger J, Degen J, Romualdi A, Deutsch U, Willecke K, Sohl G. Connexin genes in the mouse and human genome. Cell Commun Adhes 2001;8:163–165.
11. Bruzzone R, White TW, Paul DL. Connections with connexins: the molecular basis of direct intercellular signaling. Eur J Biochem 1996;238:1–27.
12. Loewenstein WR. Junctional intercellular communication and the control of growth. Biochim Biophys Acta 1979;560:1–65.
13. Guthrie SC, Gilula NB. Gap junctional communication and development. Trends Neurosci 1989;12:12–16.
14. Klaunig JE, Ruch RJ. Role of inhibition of intercellular communication in carcinogenesis. Lab Invest 1990;62:135–146.
15. Mesnil M, Yamasaki H. Cell–cell communication and growth control of normal and cancer cells: evidence and hypothesis. Mol Carcinog 1993;7:14–17.
16. Musil LS, Goodenough DA. Biochemical analysis of connexin43 intracellular transport, phosphorylation, and assembly into gap junctional plaques. J Cell Biol 1991;115:1357–1374.
17. Musil LS, Goodenough DA. Multisubunit assembly of an integral plasma membrane channel protein, gap junction connexin43, occurs after exit from the ER. Cell 1993;74:1065–1077.
18. El-Fouly MH, Trosko JE, Chang CC. Scrape-loading and dye transfer. A rapid and simple technique to study gap junctional intercellular communication. Exp Cell Res 1987;168:422–430.
19. Turner FC. Sarcomas at sites of subcutaneously implanted bakelite disks in rats. J Natl Cancer Inst 1941;2:81–83.
20. Oppenheimer BS, Oppenheimer ET, Danishefsky I, Stout AP, Eirich FR. Further studies of polymers as carcinogenic agents in animals. Cancer Res 1955;15:333–340.
21. Bischoff F, Bryson G. Carcinogenesis through solid state surface. Prog Exp Tumor Res 1964;5:85–133.
22. Karp RD. Tumorigenesis by Millipore filters in mice: histology and ultrastructure of tissue reactions as related to pore size. J Natl Cancer Inst 1973;51:1275–1285.
23. Tsuchiya T, Hata H, Nakamura A. Studies on the tumor-promoting activity of biomaterials: inhibition of metabolic cooperation by polyetherurethane and silicone. J Biomed Mater Res 1995;29:113–119.
24. Tsuchiya T. A useful marker for evaluating tissue-engineered products: gap-junctional communication for assessment of the tumor-promoting action and disruption of cell differentiation in tissue-engineered products. J Biomater Sci Polym Ed 2000; 11:947–959.
25. Nakaoka R, Tsuchiya T, Kato K, Ikada Y, Nakamura A. Studies on tumor-promoting activity of polyethylene: inhibitory activity of metabolic cooperation on polyethylene surfaces is markedly decreased by surface modification with collagen but not with RGDS peptide. J Biomed Mater Res 1997;35:391–397.
26. Brand I, Buoen LC, Brand KG. Foreign-body tumors of mice: strain and sex differences in latency and incidence. J Natl Cancer Inst 1977;58:1443–1447.
27. Musil LS, Cunningham BA, Edelman GM, Goodenough DA. Differential phosphorylation of the gap junction protein connexin43 in junctional communication-competent and -deficient cell lines. J Cell Biol 1990;111:2077–2088.
28. Lampe PD, Lau AF. Regulation of gap junctions by phosphorylation of connexins. Arch Biochem Biophys 2000;384:205–215.
29. Asamoto M, Toriyama-Baba T, Krutovskikh V, Cohen SM, Tsuda H. Enhanced tumorigenicity of rat bladder squamous cell carcinoma cells after abrogation of gap junctional intercellular communication. Jpn J Cancer Res 1998;89:481–486.
30. Moorby C, Patel M. Dual functions for connexins: Cx43 regulates growth independently of gap junction formation. Exp Cell Res 2001;271:238–248.
31. Wyatt LE, Chung CY, Carlsen B, Iida-Klein A, Rudkin GH, Ishida K, Yamaguchi DT, Miller TA. Bone morphogenetic protein-2 (BMP-2) and transforming growth factor-beta1 (TGF-beta1) alter connexin 43 phosphorylation in MC3T3-E1 cells. BMC Cell Biol 2001;2:14.
32. Laird DW, Castillo M, Kasprzak L. Gap junction turnover, intracellular trafficking, and phosphorylation of connexin43 in brefeldin A-treated rat mammary tumor cells. J Cell Biol 1995; 131:1193–1203.